Coherence effects in laser-fluorescence molecular-beam magnetic resonance

A. G. Adam, S. D. Rosner, T. D. Gaily, and R. A. Holt
The University of Western Ontario, London, Ontario N6A 3K7, Canada
(Received 19 October 1981)

New studies of Na_2 hyperfine structure (hfs) by the laser-induced-fluorescence molecular-beam magnetic-resonance technique are described which show that state selection and detection by strong optical fields can produce rf-magnetic-resonance spectra which differ drastically from the Rabi shape, even though the optical and rf fields do not act simultaneously on the molecules. We suggest that in the case of optically unresolved ground-state sublevels these effects are due to the creation of ground-state coherence by absorption and stimulated-emission cycles in the laser field, and we present a model calculation which exhibits the essential features of the observed spectra. We also give a proof that no model based only upon populations can explain the negative signals we observe.

I. INTRODUCTION

The molecular-beam magnetic-resonance method (MBMR), developed by Rabi, Kusch, and Ramsey in the 1940's, has produced an enormous amount of highly precise information about atomic and molecular fine and hyperfine structures and multipole moments.[1] The combination of this technique with laser-induced-fluorescence state selection was achieved only in 1975,[2] but it has already produced a significant body of literature describing measurements of high precision and selectivity.[3–7] The advantages of laser-induced-fluorescence molecular-beam magnetic resonance (LFMBMR) are clear: in contrast to conventional MBMR it can selectively examine a single rovibrational level, it can be applied to ionic species, and it substitutes relatively efficient laser-fluorescence detection for the typical "universal ionizer." Furthermore, in contrast to optical pumping in a cell, there are no collisions with a buffer gas or the cell walls, and there are no light shifts because the light and the rf interact with the system in spatially separate regions.

A highly schematic diagram of the technique is shown in Fig. 1. A beam of atoms, molecules, or ions (to be referred to quite generally as "molecules" in the following) intersects a cw laser beam in a region A, typically a few mm long. If the ground-state splitting is greater than the width of the optical transition, then a large population difference can be created by tuning the laser to one of the line components. Even if this is not possible, the Zeeman sublevels can be aligned (or polarized) by suitably polarized light, creating the necessary ground-state population differences. (It is characteristic of most of the experiments to date that the "optical pumping" is mainly a depletion process in which the probability of a return to the lower level of the optical transition is very small, either because this level is a highly excited metastable level of an atom or ion, or because the optically excited state can decay to many other vibration-rotation levels of a molecule.) Magnetic resonance is then used to alter the populations in the C region. These changes are detected at a second molecular-beam laser-field intersection (the B region) at which spontaneous emission is viewed by a photodetector. An rf resonance spectrum is produced by scanning the frequency while recording the difference in the B fluorescence with the rf on and off.

II. EXPERIMENTAL RESULTS

Of all the published work it appears that the original demonstration of the technique,[2] using Na_2, has been the only one in which the rf splittings were

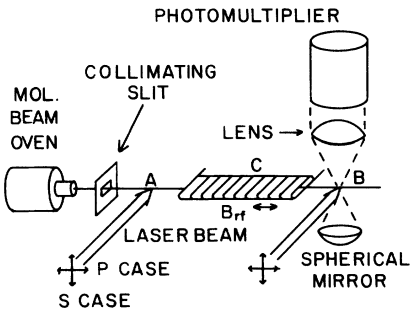

FIG. 1. Schematic view of the apparatus for a typical LFMBMR experiment.

not also optically resolved, and it was this system which we chose to reexamine in greater detail. A frequency-stabilized single-mode cw argon-ion laser operating at 476.5 nm was used to excite the $X\,^1\Sigma_g^+$, $v''=0$, $J''=28\rightarrow B\,^1\Pi_u$, $v'=6$, $J'=27$ transition in a supersonic Na_2 beam. To ensure spatially uniform pumping at the A and B regions, the laser beam was expanded to a $1/e^2$ diameter of 4.78 mm, and the Na_2 beam was collimated to have a spread in the vertical plane of ~ 2 mrad, implying a height at the B region of 1.6 mm. A 50-mW laser beam at A caused the B fluorescence to decrease to about 0.7% of its value with no A beam. In the horizontal plane the molecular-beam collimation was ~ 9.4 mrad, which produced a Doppler width of 25 MHz, chosen to be equal to the natural width of the transition (due to the 7 nsec lifetime of the $B\,^1\Pi_u$ state[8]). The transit time of the molecules in the laser beam implies an uncertainty width of 0.3 MHz; the fact that this exceeds the ground-state hyperfine structure (hfs) plays an important role in the model to be discussed below.

The ground-state hfs of Na_2 arises mainly from the electric quadrupole interaction and to a much lesser extent from the spin-rotation interaction. The hfs of an even-J'' level, such as the $J''=28$ level studied, is shown in Fig. 2. The degeneracy of the Zeeman sublevels was maintained in the experiment by canceling the ambient static magnetic field to better than 5 mG. The transitions ν_3 and ν_4, at about 110 kHz, and ν_5 and ν_6, at about 122 kHz, were chosen for study because they are strong and virtually unaffected by the Bloch-Siegert shift at practical power levels.[1] The transitions of each pair were unresolvable within the 4-kHz transit-time-limited resolution of the C region (a flattened solenoid 36.2 cm in length). Thus at low rf power one expects to see a spectrum of two reasonably well-resolved peaks, each composed of two highly overlapped Rabi line shapes.[1] As the power is increased one expects a line broadening, which is complicated by the multiplicity of M_F'' values involved.

The early experiment, carried out with the ambient magnetic field not canceled, with the fairly high rf field of 7.7 G (0-peak), and with a low-power unexpanded laser beam, gave results which seemed to agree with the above expectations. The new series of experiments, performed under the much cleaner conditions already described, has examined the changes in line shape over a broad range of rf amplitudes, as well as the effects of changing the laser power and the linear polarization from its original orientation perpendicular to the rf magnetic field (S case) to parallel (P case). The results for the P case are summarized in Figs. 3(a)–5(a). The expected twin peaks are present in Fig. 3(a), along with subsidiary Rabi wiggles, but even at the low rf amplitude of 3.5 G the peaks are significantly broader than the 4-kHz transit-time width. At higher power each peak splits into two, producing a

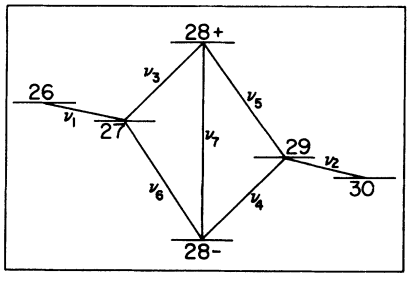

FIG. 2. Hfs of the $v''=0$, $J''=28$ level of the $X\,^1\Sigma_g^+$ electronic ground state of Na_2. Levels are labeled by the total angular momentum quantum number F''. $F''=28$ levels arising from $I=0$ and 2 are strongly mixed by the quadrupole interaction to give the levels labeled as $28\pm$.

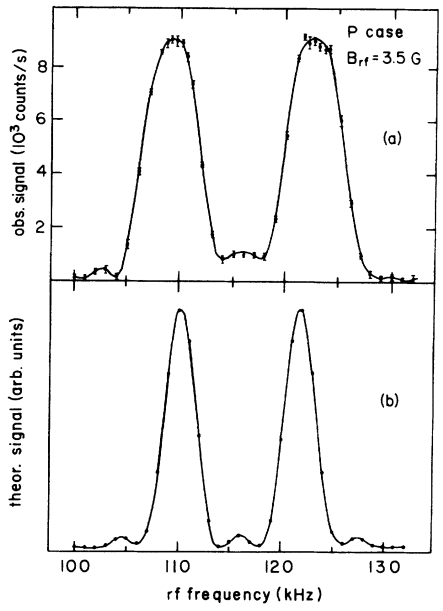

FIG. 3. (a) LFMBMR spectrum with laser polarization parallel to the rf magnetic field (P case), at an rf field of 3.5 G 0-Peak. Laser power at the A and B regions was 46 and 11 mW, respectively. Solid line is a smooth curve through the data. Error bars were estimated by taking eight 10-sec measurements at each frequency (using a frequency scanning pattern designed to minimize systematic errors). (b) Theoretical prediction for comparison with (a). See text for details of the model.

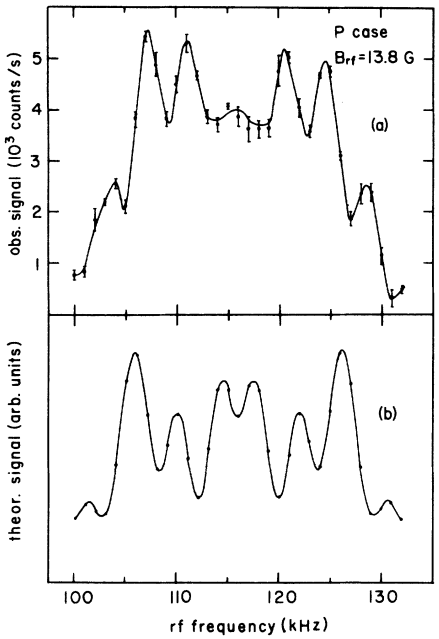

FIG. 4. Same as Fig. 3, at an rf field of 13.8 G.

curve somewhat resembling a Rabi line shape[1] at twice the optimum rf amplitude [see Fig. 4(a)]. The dependence of the signal "at resonance" vs rf amplitude, shown in Fig. 5(a), shows oscillations characteristic of the Rabi two-level formula.

The results for the *S* case are remarkably different and quite unexpected. At low rf power the resonance curve acquires pronounced negative peaks, as shown in Fig. 6(a). Figure 7(a) shows the signal at a fixed frequency of 110 kHz plotted against rf amplitude, with a laser power of 50 mW at the *A* region. As the laser power is reduced, this curve retains all of its features in the same locations, but the extrema become progressively shallower. Lowering the laser power also has the effect of rendering the valley between the 110- and 122-kHz peaks in the rf spectrum less pronounced. The complete rf spectra in Fig. 8 show that at the 6.2-G zero crossing of Fig. 7(a) the signal *at all frequencies* is in fact not much above the noise. Finally, it should be noted that there is no simple correspondence between the frequencies of the peaks in the *S* and *P* cases.

III. THEORETICAL MODELS

In the discussions of the theoretical modeling of LFMBMR in the literature it is always assumed that one need only consider populations and the

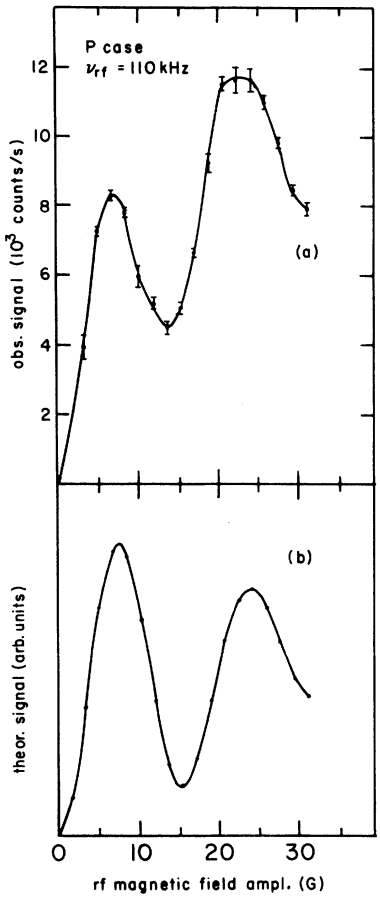

FIG. 5. (a) Experimental and (b) theoretical dependence of *P*-case LFMBMR signal upon rf field amplitude, for a fixed rf frequency of 110 kHz.

probabilities of their transfer among states by the optical and rf fields in the *A*, *B*, and *C* regions.[2–7] However, such a model must necessarily produce *positive* signals if the light polarization is the same at *A* and *B*. For any pair of hyperfine states, the population of the state that absorbs the light more strongly will be depopulated relative to the other at the *A* region. A resonant rf field will therefore always effect a net transfer of population to the less populated (and hence more strongly absorbing) state and thus produce an increase in fluorescence at *B*. A formal proof that the signals predicted by a population model cannot be negative is given in the Appendix.

We propose to explain the new observations by an amplitude model in which coherence between ground-state sublevels is created by laser-induced absorption and stimulated emission. This can be accomplished with a given incoming and an identical outgoing photon only if the hyperfine splitting

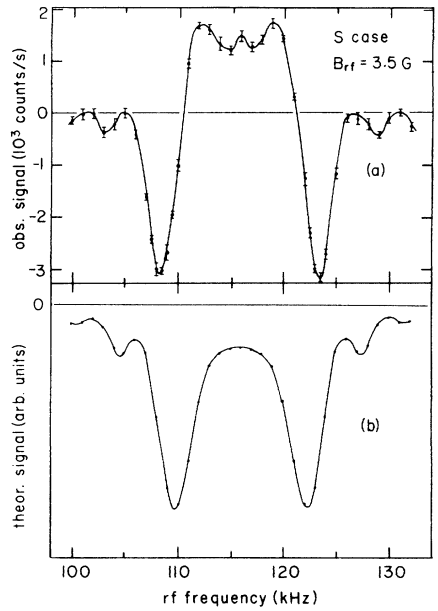

FIG. 6. (a) Experimental and (b) theoretical LFMBMR spectra with laser polarization perpendicular to rf magnetic field (S case), at an rf field of 3.5 G. Laser power at A and B regions was 50 and 7 mW, respectively.

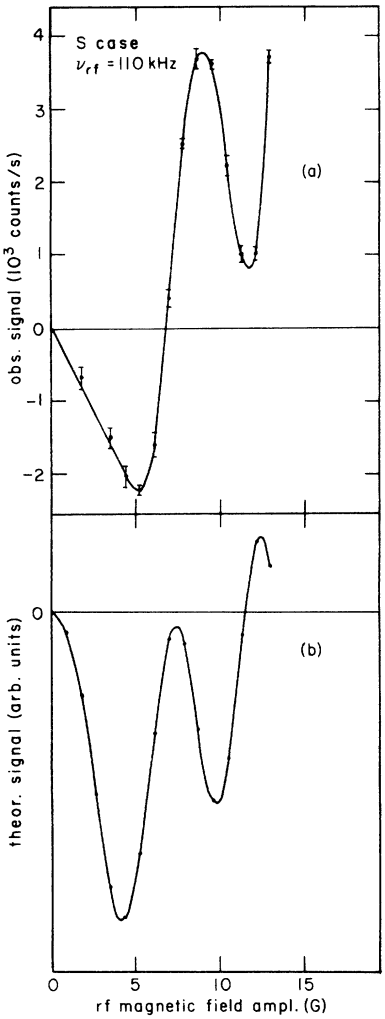

FIG. 7. (a) Experimental and (b) theoretical dependence of S-case LFMBMR signal upon rf field amplitude, for a fixed frequency of 110 kHz.

is smaller than $1/t_A$, where t_A is the transit time across the A region. Of course the "final" states of the molecule after the A region are different in this process, and no interference would be observed with a single laser-fluorescence region. In general, there are two conditions necessary for there to be nonvanishing interference effects between a pair of quantum paths: (i) they must have identical initial and final states of the entire system (molecule plus optical and rf fields), and (ii) the effects of averaging must not wash out the interference terms in practice. (In this model the important averages are over the velocity distribution of the rf field at the time of entry of a molecule into an interaction region.)

In our calculations we have used a semiclassical treatment of the radiation field mode driven by the laser; this is known to lead to the same results as a fully quantized treatment in such strong-field situations.[9] The coupling between the molecules and the optical radiation field is thus taken to be

$$\langle i \mid \mathscr{H}_c \mid j \rangle = \mu_{ij}(2I/c\epsilon_0)^{1/2}\{\tfrac{1}{2}\exp[i(\omega_l t+\phi_l)]+\text{c.c.}\}\ , \tag{1}$$

in which i is any state of the $X\,^1\Sigma_g^+$ level, j is any $B\,^1\Pi_u$ state, μ_{ij} is the electric dipole matrix element (which we estimate from the measured lifetime and calculated branching ratios), and I, ω_l, and ϕ_l are the intensity, frequency, and phase of the laser, respectively. Because a molecule which absorbs a laser photon has only a 3% chance of returning to the initial rotation-vibration level by *spontaneous* emission, we have neglected this process in a first approximation. Spontaneous emission to all other levels is treated by introducing a non-Hermitian damping Hamiltonian[10,11]:

$$\langle i \mid \mathscr{H}_d \mid j \rangle = \begin{cases} -i\hbar(\gamma/2), & i=j \text{ for any } B\,^1\Pi_u \text{ state} \\ 0, & \text{otherwise}\ . \end{cases}$$

The damping constant γ is equal to the inverse of the natural lifetime of the B state.

The rotating-wave approximation[9] is then made by dropping the complex conjugate "counter-rotating" term in Eq. (1). This allows us to transform away all explicit time dependence from the Hamiltonian by means of the unitary transformation

$$\langle i \mid \mathscr{U}(t) \mid j \rangle = \begin{cases} 1, & i=j \text{ for any } X\,{}^1\Sigma_g^+ \text{ state} \\ \exp[-i(\omega_l t+\phi_l)], & i=j \text{ for any } B\,{}^1\Pi_u \text{ state} \\ 0, & \text{otherwise} . \end{cases}$$

We can then solve for the (nonunitary) time-evolution operators in the A and B regions, V^A and V^B, by standard matrix techniques. The unitary time-evolution operator U^C for the rf region is obtained in the same way except for the absence of any significant spontaneous rf emission.

The probability of finding a molecule in state i after the B region is given by

$$P_i(B)=\sum_l \left| \sum_{j,k} V^B_{ij} U^C_{jk} V^A_{kl} \right|^2 , \tag{2}$$

where j, k, and l run over all the states of the particular electronic ground-state rovibrational level. The corresponding probability $P_i(C)$ of finding a molecule in state i after the C region is given by Eq. (2) with V^B replaced by the identity. The spontaneous optical emission $\mathscr{F}$ at B is calculated as the difference of these probabilities,

$$\mathscr{F}=\sum_i [P_i(C)-P_i(B)] , \tag{3}$$

which equals the number of molecules which have "disappeared" via spontaneous decay of $B\,{}^1\Pi_u$ states to other $X\,{}^1\Sigma_g^+$ rovibrational levels. The signal is then the difference in this fluorescence $\mathscr{F}$ with the rf on and off, averaged over the velocity distribution of the molecular beam[12,13] and over the phase of the rf field seen by a molecule as it enters the C region. (The phase of the optical field has no effect because it only appears in the amplitudes of $B\,{}^1\Pi_u$ levels, and these are negligible anywhere outside of the laser interaction regions.)

In order to clarify the origin of coherence effects, consider a simple model for the S case consisting of only the five states shown in Fig. 9. The ground

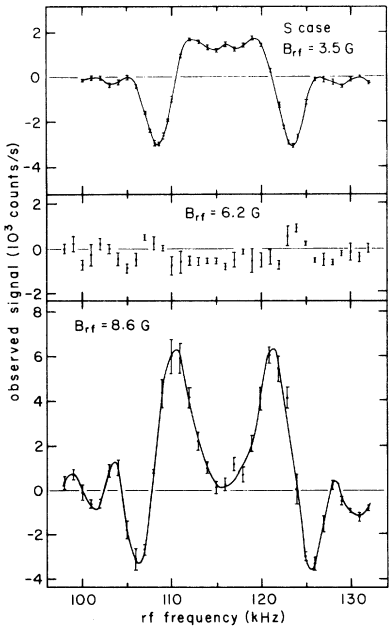

FIG. 8. S-case LFMBMR spectra at various rf magnetic fields. Laser power at A was 50, 25, and 65 mW for (a), (b), and (c), respectively.

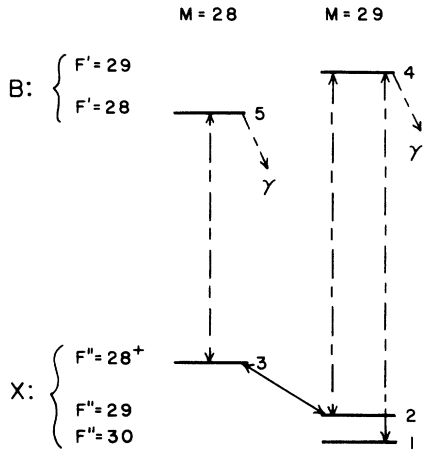

FIG. 9. Five states of a simple model labeled by F, the total angular momentum of the molecule, and M, its z component. Dashed lines indicate optical transitions, while the solid line represents an hf transition driven by the rf magnetic field. X and B label the relevant electronic states of the molecule. Spontaneous-emission decay rate is denoted by γ.

states labeled 1 and 2 are connected optically to the same excited state, 4, while ground state 3 is connected to a different excited state, 5. The rf is resonant only for transitions between states 2 and 3. Consider a molecule initially in state 1. After the A region, if the molecule has not fluoresced, it will be left in a linear combination of states 1 and 2 as a result of absorption and stimulated emission. With no rf field in the C region, this molecule will arrive at the B region in a new linear combination of states 1 and 2 as a result of the action of the hyperfine Hamiltonian. (When the calculated signals are averaged over the velocity distribution, this effect destroys many coherence terms between hyperfine levels differing in energy by ~ 100 kHz. For states such as 1 and 2, which differ by ~ 5 kHz, the coherence remains.)

The calculation of the fluorescence at B then proceeds from Eqs. (2) and (3). Even though Eq. (2) is equivalent to a sum over all orders of perturbation theory, it is nevertheless instructive to examine diagrammatically a typical pair of interfering quantum paths which would contribute to the signal in a perturbation treatment. Figure 10 shows such a pair for the case of a molecule which begins in state 1. The expression for the fluorescence at B will contain an interference term arising specifically from the fact that the molecule is in a linear superposition of states 1 and 2 after the A region. In other words, the probability of absorbing a photon at B to reach state 4 is *not* the same for a given *linear combination* of states 1 and 2 as it would be for a *mixture* with the same diagonal density-matrix elements. Thus the fluorescence at B can be greater or smaller than that predicted by a population model. Consider now a resonant rf field applied in the C region causing transitions between states 2 and 3. This will reduce the coherence effect because state 3 cannot be optically excited to the same $B\,^1\Pi_u$ state as can either 1 or 2. In both this model and in the considerably more elaborate one discussed below, the B fluorescence with no rf is predicted to be greater than the incoherent value, and thus the effect of small-amplitude rf is to reduce the fluorescence, causing a negative signal. In a more complete model, one expects the signal to become positive at rf fields of large amplitude because molecules can be transferred to states of low $|M_F''|$ which have much larger optical-absorption matrix elements.

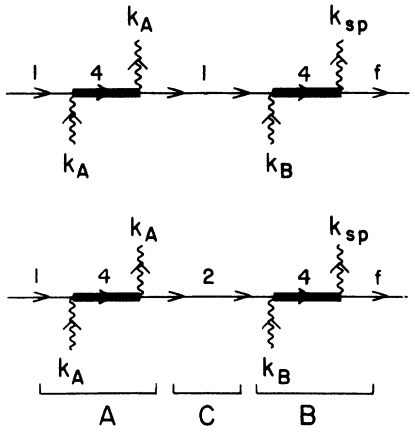

FIG. 10. Quantum paths which contribute coherently to the predicted signal for the simple model of Fig. 9. Thin straight lines represent a molecule in the ground state, thick lines represent a molecule in the electronic excited state, and wavy lines represent a photon in state k. Label f refers to any rovibrational level except $v''=0$, $J''=28$.

The $v''=0$, $J''=28$ level has 342 hyperfine states, counting all possible values of F'' and M_F''. If the axis of quantization is chosen parallel to the electric field vector of the light, only $\Delta M_F=0$ optical transitions are allowed and the optical pumping problem subdivides into 31 much smaller problems, one for each possible $|M_F''|$ value. In the P case discussed earlier, this same simplification occurs for the rf problem. In addition, consideration of the M_F''-dependence of the optical matrix elements shows that only a few states with the very largest $|M_F''|$ values have any significant amplitude in the state vector after the A region; molecules in states of small $|M_F''|$ are completely pumped away to other rovibrational levels. In the S case, however, rf transitions with $\Delta M_F''=\pm 1$ are allowed, coupling all 342 states together. The molecules in states of large $|M_F''|$ are transferred "inward" fairly slowly at the rf amplitudes used in the experiment, so that most of the states of small $|M_F''|$ can be ignored in this case as well. Nevertheless, the computational labor involved in the S case is considerably greater than that in the P case, and a less realistic model has to be employed.

Figures 3(b)—5(b) shows the results of a calculation for the P case which includes all states with $M_F''\geq 25$. While the overall shape of the rf spectrum compares very well with experiment, the linewidth is about $\frac{2}{3}$ of the experimental value. The hfs parameters eqQ and c used in this and all of the computations discussed below were taken from the high-frequency data of Ref. 2. One could obtain slightly better agreement of the predicted and mea-

sured peak separations by choosing optimum values for these hfs constants. The model shows that for the dominant $M_F''=28$ and 27 contributions to the signal, the phase and velocity averaging removes almost all coherence terms, giving nearly the same result as a population model. The S-case curve shown in Fig. 6(b), based on a model with eight states of large M_F'', predicts the dominant negative peaks but has the wrong sign in the central region. The shift of the peak centers between the S and P cases is present in these models. The oscillatory behavior of the signal vs rf amplitude at a fixed frequency is reproduced by the calculation; positions of the extrema agree within 8% in the P case (Fig. 5) and 20% in the S case (Fig. 7).

Besides the limitation on the number of states used, a possible reason for the remaining disagreement between experiment and theory is that several effects have been omitted from the model which could enhance the contribution of states with smaller $|M_F''|$ values. These include averaging over the geometry of the laser-molecular-beam interaction regions (Doppler shifts, transit-time variations), and anisotropic distribution of the fluorescence at B (angular correlations). An increased contribution from the states omitted in the P case would broaden the line because the matrix elements of the rf Hamiltonian get larger with decreasing $|M_F''|$. Another limitation of these models is the assumption that the initial density matrix of the molecules before they reach the A region is isotropic. There is some evidence that this is not generally true of supersonic dimer beams, especially at high stagnation pressures.[14] The M dependence of this effect appears to be much more gradual than that of the laser-induced depletion in the A region; thus, in view of the crude nature of the present model, we have not included this refinement in the calculation.

In addition to further study of these (and possibly other) omitted effects, we plan to observe hyperfine transitions in a level of much lower J'' using a new laser system, thus reducing the number of states involved. Once the line shapes produced by LFMBMR are completely understood, the full precision of this powerful technique will be achievable.

ACKNOWLEDGMENTS

We would like to thank the Natural Sciences and Engineering Research Council of Canada for financial support, and we wish to thank I. Schmidt, H. Walter, and J. Keyser for expert technical assistance.

APPENDIX

The statement of Sec. III that a population model yields only positive signals can be demonstrated as follows. If there are n molecular states in the ground level, then let A_i be the probability that a molecule in the ith state does *not* fluoresce in the A region and B_i be the corresponding probability for the B region. Then, if P_{ji} is the probability of an $i\rightarrow j$ rf transition in the C region, the net signal S is given by

$$S=\sum_i\sum_j(1-B_j)P_{ji}A_i-\sum_i(1-B_i)A_i\ ,$$

in which the first term is the fluorescence at B with the rf on and the second is with the rf off. After a little algebraic manipulation this may be rewritten as

$$S=\sum_i\sum_{j>i}(B_j-B_i)(A_j-A_i)P_{ji}\ ,$$

making use of the fact that $P_{ij}=P_{ji}$ and that

$$\sum_j P_{ji}=1,\quad i=1,\ldots,n\ .$$

We note finally that if the light polarization is the same at the A and B regions then the factors (B_j-B_i) and (A_j-A_i) must have the same sign, and since each term in the sum is thus non-negative (P_{ji} is a probability), we conclude that $S\geq 0$.

[1]N. F. Ramsey, *Molecular Beams* (Clarendon, Oxford, 1956).

[2]S. D. Rosner, R. A. Holt, and T. D. Gaily, Phys. Rev. Lett. 35, 785 (1975).

[3]W. Ertmer and B. Hofer, Z. Phys. A 276, 9 (1976).

[4]S. D. Rosner, T. D. Gaily, and R. A. Holt, Phys. Rev. Lett. 40, 851 (1978).

[5]W. J. Childs, O. Poulsen, and L. S. Goodman, Phys. Rev. A 19, 160 (1979); Opt. Lett. 4, 35 (1979); 4, 63 (1979); W. J. Childs, O. Poulsen, L. S. Goodman, and H. Crosswhite, Phys. Rev. A 19, 168 (1979); W. J. Childs and L. S. Goodman, *ibid.* 20, 1922 (1979); 21, 1216 (1980); Phys. Rev. Lett. 44, 316 (1980).

[6]A. Yokozeki and J. S. Muenter, J. Chem. Phys. 72,

3796 (1980).
[7]U. Kötz, J. Kowalski, R. Neumann, S. Noehte, H. Suhr, and K. Winkler, Z. Phys. A 300, 25 (1981).
[8]W. Demtröder, W. Stetzenbach, M. Stock, and J. Witt, J. Mol. Spectrosc. 61, 382 (1976).
[9]L. Allen and J. H. Eberly, *Optical Resonance and Two-level Atoms* (Wiley, New York, 1975).
[10]V. Weisskopf and E. Wigner, Z. Phys. 63, 54 (1930).
[11]W. Heitler, *The Quantum Theory of Radiation* (Clarendon, Oxford, 1954).
[12]T. D. Gaily, S. D. Rosner, and R. A. Holt, Rev. Sci. Instrum. 47, 143 (1976).
[13]K. Bergmann, U. Hefter, and P. Hering, J. Chem. Phys. 65, 488 (1976).
[14]M. P. Sinha, C. D. Caldwell, and R. N. Zare, J. Chem. Phys. 61, 491 (1974).